Journal of Materials Chemistry A

Accepted Manuscript

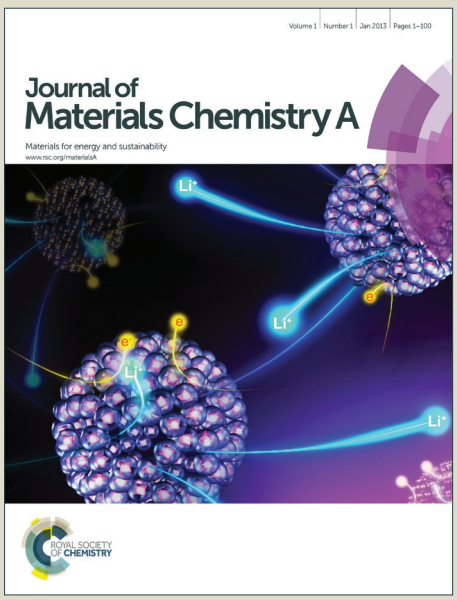

ROYAL SOCIETY OF CHEMISTRY

www.rsc.org/materialsA

Journal Name

RSCPublishing

COMMUNICATION

Novel oxygen transport membranes with tunable segmented structures

Cite this: DOI: 10.1039/xoxxoooooox

Jong Hoon Joo[a], Kyong Sik Yun[b], Chung-Yul Yoo[a] and Ji Haeng Yu[a,*]

Received ooth January 2012,
Accepted ooth January 2012

DOI: 10.1039/xoxxoooooox

www.rsc.org/

A novel oxygen permeation membrane with a tunable segmented configuration obtained by employing tape casting technique has been developed. According to this new structure, the membrane consists of a robust fluorite oxide matrix and electron conducting perovskite oxide segments. Mixed electron-ion conduction in the membrane can be optimized by controlling a number of the electron conducting segments. This new concept of the membrane with high oxygen permeability is proposed for the industrial oxygen production.

Ceramic-based ion transport membranes with high oxygen permeability have received increasing attention as promising alternatives to cryogenic distillation to supply pure oxygen to power plants with CO_2 capture based on oxy-fuel combustion.[1-3] The thermo-chemical and mechanical stability of the membranes are the main issues, which limit their practical application.[4-6] Due to their high oxygen permeability, most studies on ion transport ceramic membranes have focused on perovskite (ABO_3) materials such as $Ba_{0.5}Sr_{0.5}Co_{0.8}Fe_{0.2}O_{3-\delta}$ (BSCF), which contain rare and alkaline earth metals at the A-site and a transition metal at the B site.[7-11] However, the chemical instability of these materials under operation in the presence of gases like CO_2 and H_2O limits their practical applications. In addition, their high thermal and chemical expansion can cause cracking and delamination of ceramic membranes.[12,13] In order to overcome these issues, focus has shifted to the development of dual-phase membranes consisting of a fluorite material with a high ionic conductivity and chemical stability, which acts as the oxygen ion conductor, and a perovskite, which acts as the electron/ion conductor. Composite membranes can benefit from the contribution of each phase and overcome the limitations of perovskite materials.[14-16] However, inter-diffusion of the phase components during sintering cannot be avoided, which can lead to low oxygen permeation fluxes in the dual-phase membrane.[17-19]

Recently, a new concept has been proposed for the oxygen separation membranes that use doped CeO_2 with Pt layers on the feed and permeate side, which are externally short-circuited with Ag paste.[20] The lack of electron conduction in doped-CeO_2 (internal current) is compensated by the external current via the noble metal paste. This type of membrane can be considered as a short-circuited solid oxide fuel cell (SOFC), which is robust in atmosphere containing CO_2 and/or H_2O. More recently, researchers have reported an internally short-circuited CeO_2-based membrane with an Ag wire implanted inside a hole made through the doped-CeO_2.[21] However, the use of excessive noble metal within the membranes limits their wide-scale industrial use because of the excessive costs. Further, the thermal expansion coefficient (TEC) mismatch between the fluorite material ($Ce_{0.9}Gd_{0.1}O_{2-\delta}$, TEC ~ 11×10^{-6} K^{-1})[22] and the noble metal (Ag, TEC ~ 19×10^{-6} K^{-1}) can cause delamination and material fracture at the interface, leading to a reduction in the long-term performance. In addition, drilling the ceramic to fabricate a hole in the fluorite is unsuitable because the process is both complex and time-consuming. Another approach to devoid of the use of noble metal has also been reported.[23] $La_2NiO_{4+\delta}$ was adopted to replace the noble metal. However, Ag was still used to form the external short-circuit and the disadvantage of this configuration is that the scale-up is limited because of the increase in the lateral resistance along the external short circuit.

Herein, we propose a novel structure for oxygen permeation membrane with a tunable segmented configuration obtained by tape casting technique. According to this new concept, the membrane consists of a robust fluorite material with a stable electron conducting oxide (i.e., a non-noble metal). The advantage of this proposed membrane is that the mixed conductivity of the membrane can be optimized by controlling the area of the ionic and electronic phases. In addition, SOFC tests were carried out to demonstrate the concept of the novel membrane, which combines the progress in SOFC and mixed conducting membranes. To the best of our knowledge, this is the first attempt to experimentally apply the results of the SOFC tests (cell voltages as a function of current density) to the oxygen permeation membrane. Our investigation clearly demonstrates that the electron conducting oxide enables the permeation of oxygen through the fluorite phase. Further, large area membranes can be developed because the area of the fluorite and electronic phases can be tuned by the tape casting technique, as shown in Fig. 1.

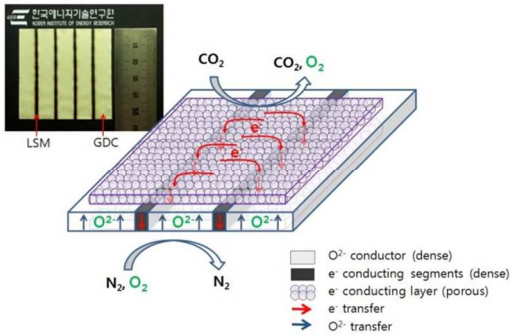

Fig. 1 Schematic drawing and image of the segmented oxygen permeation membrane

In this study, Gd-doped ceria (GDC) and strontium-doped lanthanum manganite (LSM) are used as the oxygen ion conductor and stable electronic conductor, respectively. GDC and LSM are commonly used as SOFC materials because they possess sufficient chemical stability. In addition, the difference in the average TECs of GDC and LSM in air is as low as 2%[24] which indicates good stability of the membrane under thermal cycling conditions.

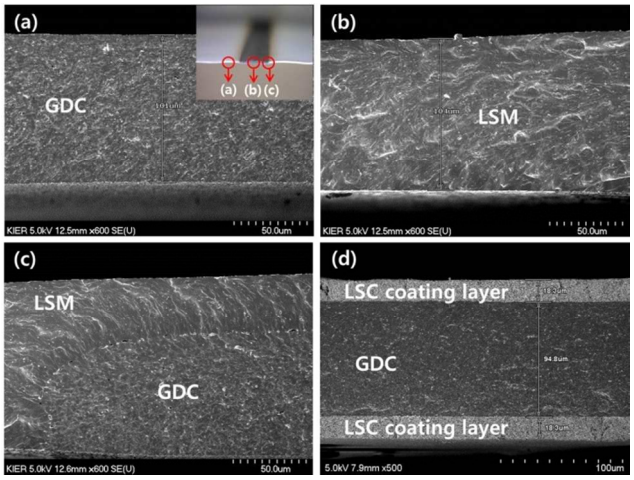

Fig. 2 SEM micrographs of the membrane, images of the cross section of sintered (a) GDC, (b) LSM, (c) GDC/LSM interface, and (d) SEM image of the GDC coated by LSC layers

Fig. 2 shows the cross-sectional scanning electron microscopy (SEM) images of the segmented membrane. The thickness of the densified GDC and LSM is ~ 100 μm. The gas tightness of the membranes was determined by nitrogen permeation, which indicates that GDC and LSM are fully dense with good adhesion between the GDC/LSM interfaces. The gas leakages were no more than 0.2 % for all the permeation experiments. Fig. 2 (d) shows that strontium-doped lanthanum cobaltite (LSC) is coated on both sides of the membrane. The porous electron-conducting layers, which can be assigned as the cathode and anode adapted from the configuration of SOFC, are connected by the LSM conductor. In this manner, mixed ionic-electronic conducting can be achieved via oxygen ion transport through the GDC and electronic conduction along the LSM, avoiding the inter-diffusion of the two phases during the powder mixing.

In order to verify the workability of the new membrane, which consists of a fluorite material with segmented electron conducting oxide, GDC-based membranes with different numbers of electron conducting segments ($La_{0.7}Sr_{0.3}MnO_3$) were tested for oxygen permeation under an air/helium gradient as shown in Fig.3.

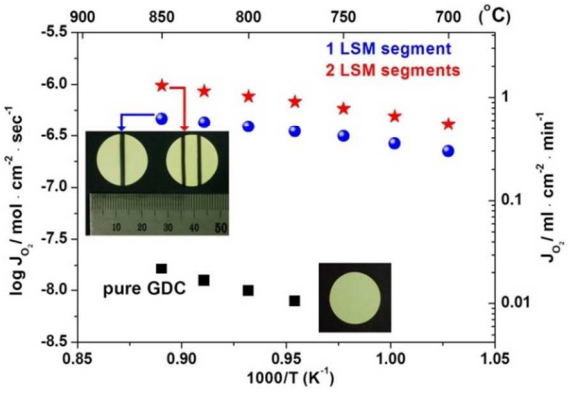

Fig. 3 Temperature dependence of the oxygen fluxes of the segmented and pure GDC membranes (membrane thickness~ 100 μm).

To obtain accurate activation energies for the oxygen permeability of the membrane, the oxygen partial pressure gradient was fixed at 2.1 $\times 10^{-1}$ atm/3.3 $\times 10^{-4}$ atm. Oxygen transport occurs by ionic diffusion through the GDC accompanied by conduction of electrons for charge compensation. When permeation is controlled by bulk diffusion, the oxygen flux is proportional to the ambipolar conductivity.

$$J_{O_2} = \frac{RT}{16F^2L}\int_{\ln P''_{O_2}}^{\ln P'_{O_2}} \frac{\sigma_{el}\sigma_{ion}}{\sigma_{el}+\sigma_{ion}} d\ln P_{O_2} \quad (1)$$

In the above equation, L is the membrane thickness, σ_{el} is the electronic conductivity, σ_{ion} is the ionic conductivity, T is the temperature, R is the gas constant, F is the Faraday constant, and Po_2 is the oxygen partial pressure. As expected, the pure GDC membrane with LSC active layers coating exhibited the lowest oxygen permeability because of the lack of electronic conductivity. In the case of the segmented membrane, the oxygen permeation was dramatically increased because of electronic conduction in the segmented electron conducting oxide. Since the ionic conductivity of LSM (~10^{-7} S/cm)[25] is about six orders of magnitude lower than that of GDC (~10^{-1} S/cm)[26] at 800 °C in air, the permeability through LSM can be negligible. The oxygen flux through GDC with the two electron conducting oxides was 1.31 ml/cm^2·min, which is in contrast to the very low flux value of 0.02 ml/cm^2·min through pure GDC at 850 °C. The dramatic enhancement in the oxygen flux indicates that the mixed ionic-electronic conduction is achieved in the segmented membrane via the electronic conduction along the LSM and porous LSC layers. This also demonstrates that an internal short-circuit could be constructed in the membrane without using a noble metal. The effect of the number of electron conducting oxides on the permeability of the membranes was also confirmed, as shown in Fig.3. The overall oxygen transport through the segmented membrane comprises of *i*) the electronic conduction in the LSM electron-leading oxide, *ii*) the ionic conduction of GDC, *iii*) the surface exchange kinetics at the LSC/GDC interface, and *iv*) the electronic conduction of the LSC coating layer. The activation energy values of the electronic conductivity in LSM, the electronic conductivity in LSC, the ionic conductivity in GDC, and the surface exchange rate on LSC/GDC are 0.07 eV,[27] 0.04 eV,[28] 0.6 eV,[15] and 1.1 eV,[29] respectively. Based on our permeation results, the apparent activation energies for permeation through the membrane with one and two electron conducting oxides were calculated to be 0.45 eV and 0.54 eV, respectively. This change in the activation energy clearly indicates that the electronic conduction in both LSM and LSC coating layers still partly contributes to the oxygen transport of

the segmented membrane in combination with the GDC ionic conduction and the surface exchange kinetics at the LSC/GDC interface. If the oxygen surface exchange on the GDC is negligible and the electronic conduction is dominant in the membrane, the activation energy of oxygen permeation through GDC should be close to that (≈ 0.6 eV) of GDC ionic conductivity. Thus, it is possible to further enhance the permeability by optimizing the area of the electron conducting oxide or thickness of the porous coating layer.

SOFC test was also performed to verify the theoretical oxygen flux of the segmented membrane. The porous LSC layers, which correspond to the cathode and anode in the SOFC, were coated on both sides with pure GDC. The thickness of the GDC is ~ 100 μm, which is similar to the thickness of the segmented membrane. Pt paste and Pt mesh were used as the current collectors. In this symmetric cell, the oxygen ion is transferred from the cathode to the anode by the following equation.

$O_2 + 4e^- \rightarrow 2O^{2-}$ (high oxygen pressure side: air)
$2O^{2-} \rightarrow O_2 + 4e^-$ (low oxygen pressure side: He)

Thus, the number of oxygen ion permeating through GDC could be calculated from the current by the following equation.

$$I = 4F \times J_{O_2} \quad (2)$$

In the above equation, I is the current density (A/cm^2), F is the Faraday constant (96485 Coulombs), and J_{O_2} (mol/cm^2·sec) is the oxygen flux. According to this equation, a current density of 1 A/cm^2 corresponds to an oxygen flux of 3.48 ml/cm^2·min. In theory, the maximum current value at 0 V through the external wire in the SOFC configuration corresponds to the maximum oxygen permeability through the GDC electrolyte. The oxygen permeation flux of the segmented membrane might be lower than the corresponding current density at 0 V because the current flow encounters a bottleneck at the LSM and LSC coating layers.

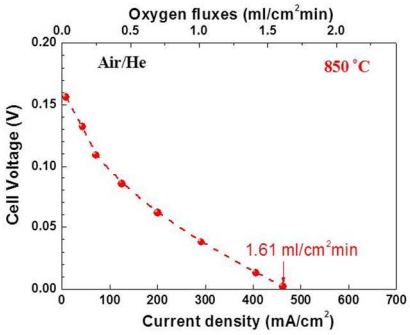

Fig. 4 Cell voltages as a function of current density for symmetric cell consisting of LSC electrodes and 100-μm-thick GDC electrolyte.

The cell voltages for the SOFC as a function of the current density are presented in Fig. 4. The open-circuit voltage (O.C.V.) for air/He is 0.156 V at 850 °C. Under this condition, the maximum current density in the SOFC is 460 mA/cm^2 and this value is equivalent to the oxygen flux of 1.61 ml/cm^2·min. From this relationship, the theoretical maximum oxygen flux can be estimated from the maximum current in the SOFC mode. Based on these results, the oxygen flux of 1.31 ml/cm^2·min at 850 °C in the segmented membrane with a thickness of 100 μm and LSC layer could be enhanced to up to 1.61 ml/cm^2·min by optimizing the electronic conduction of the segmented membrane. In order to evaluate the contributions of the ohmic and interfacial polarization resistances, impedance analysis was performed. The electrochemical impedance spectra of the symmetric SOFC cell were acquired at different cell voltages.

Fig. 5 shows the representative Nyquist plot obtained at 850 °C. The impedance spectra were composed of two semicircles; one was present at the high-frequency regime and the other was at the low-frequency regime (6Hz to 0.01 Hz). In addition, a non-zero axis intercept was present at high frequency. The intercept value can be assigned as the ionic resistance of GDC.

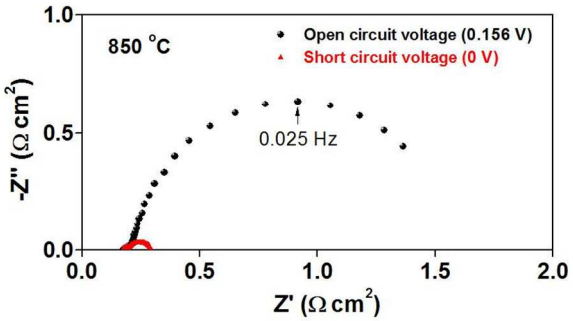

Fig. 5 Impedance spectra of the symmetric cell measured at OCV (black circle dots) and at a short circuit voltage of 0 V (red triangle dots)

The low-frequency semicircle is significantly affected by the applied cell voltage. Generally, the applied bias can affect the defect concentration of the electrode and/or the concentration of charged oxygen species on the surface. Therefore, it is reasonable to assume that this semicircle is related to the oxygen surface exchange kinetics. However, further study is required to elucidate whether low-frequency semicircle is related to the oxygen in- or ex-corporation mechanism. If the thickness of the GDC decreases to 10-20 μm, which is the dimensions usually employed in a conventional supported cell, the Ohmic resistance is expected to become much smaller than the current value and interfacial polarization resistances can be expected to dominate the permeation performance. Based on the results of the impedance in the SOFC cell, the ideal contributions of ohmic and interfacial resistances in the segmented membrane could be easily evaluated. To the best of our knowledge, this is the first report to experimentally employ the SOFC results to the oxygen permeation membrane. Preliminary stability test of the segmented membrane was performed in the presence of CO_2 at 700 °C as shown in Fig. 6. For comparison, a typical perovskite membrane $Ba_{0.5}Sr_{0.5}Co_{0.8}Fe_{0.2}O_{3-\delta}$ (~ 100 μm in thickness) was also tested using 50% CO_2 in He as the sweep gas. The oxygen flux was reduced with the addition of 50% CO_2 in the sweep gas. This decreased permeability in the presence of CO_2 could be explained by the CO_2 adsorption by the membrane surface which deteriorates the oxygen surface exchange.[20,21] However, when the sweep gas was shifted back to pure He, the oxygen flux nearly recovered to the original values. On the other hand, the BSCF membrane could not maintain the oxygen flux after switching the sweep gas from CO_2 containing gases to pure He.

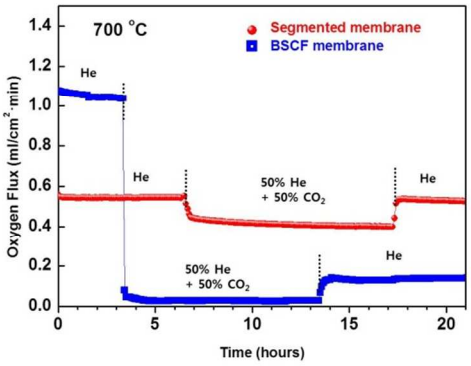

Fig. 6 Short-term oxygen permeation test of the segmented membrane and the BSCF membrane under He and 50% CO_2 in He conditions.

The oxygen permeability of BSCF was significantly deteriorated by carbonate formation due to the reaction between Ba/Sr and CO_2. The segmented membrane exhibits highly stable oxygen fluxes compared to the BSCF in He and in the presence of 50% CO_2. Even though LSC is used as the electronic-coating layer in the membrane, the chemical instability of LSC in an environment containing CO_2 has negligible impact on the stability of the segmented membrane. Further enhancement of the stability is expected by adopting CO_2 tolerant coating layers such as cobalt free $SrFe_{0.8}Nb_{0.2}O_{3-\delta}$[30] or GDC/$NiFe_2O_4$[31] composite.

Conclusions

A novel oxygen permeation membrane with a tunable segmented structure obtained by tape casting is successfully demonstrated. In this noble-metal free membrane, mixed electronic-ionic conductivity can be optimized by controlling the area of the fluorite and stable electronic oxides. In addition to demonstrating that the electron conducting oxide enables oxygen permeation through the fluorite material, with this work the progress in SOFC can be applied to the fabrication of oxygen separating membrane, which opens up a new direction to design robust ceramic-based oxygen permeation membranes.

Experimental Section

The segmented membranes were fabricated using tape casting and tape lamination techniques. To increase the sinterability of GDC, 2.5 mol% Ga-doped GDC powder was prepared by ball milling commercial GDC powder ($Ce_{0.9}Gd_{0.1}O_{2-\delta}$, Anan Kasei, Japan) and Ga_2O_3 powder (High Purity Chemicals, Japan) for 24 h. Powders of GDC and LSM ($La_{0.7}Sr_{0.3}MnO_{3-\delta}$, Kceracell, Korea) were ball-milled for 24 h with appropriate amounts of dispersant, binder, plasticizer and solvent. Tape casting of the film was carried out using a tape caster in which the slurry was coated onto a polyethylene carrier film through a lip. In order to form the segmented structure containing GDC and LSM, sheets of GDC and LSM were stacked and laminated at 70 °C for 20 min under a pressure of 10 MPa. The sample was then co-sintered at 1350 °C for 4 h to densify the membrane. $La_{0.6}Sr_{0.4}CoO_{3-\delta}$ (LSC, Kceracell, Korea) slurries were prepared by mixing the composite powder with an organic solution to form the porous electronic conducting layer. The LSC slurry was brush painted on both sides of the sintered membrane, which was subsequently fired at 1000 °C for 3 h in air. The oxygen permeation flux through the membrane was measured with a gas chromatograph (YoungLin, ACME 6000). The membranes were glass-sealed onto an alumina tube for undertaking the permeation test. Dry air (0.21 atm) was used as the feed gas with a flow rate of 400 ml/min. High purity He (99.999%) was used as the sweeping gas to create an oxygen partial pressure gradient. The gas leakages were no more than 0.2 %. The corresponding amount of oxygen leakage was subtracted based on the N_2 signal when the oxygen permeation flux was calculated. To construct the symmetric cell for the SOFC test, LSC slurry was brush painted on both sides of the sintered GDC, which was then fired at 1000 °C for 3 h. Pt paste (No.6082, Engelhard, USA) was brush painted and subsequently Pt meshes were attached at 800°C for 1h on the LSC electrodes as current collectors. An electrochemical interface (Solartron, SI 1287, UK) and impedance analyzer (Solartron, SI 1260, UK) were used to obtain the impedance spectra and current versus cell potential. The microstructure of the membranes was observed by a scanning electron microscopy (SEM, Hitachi, Japan).

Acknowledgements

This work was conducted under the framework of Research and Development Program of the Korea Institute of Energy Research (KIER) (B3-2437). The authors are grateful to Jae Hyeong Ahn for fruitful discussions.

Notes and references

[a] *Advanced Materials & Devices Laboratory, Korea Institute of Energy Research, 152 Gajeong-ro, Daejeon 305-343, Republic of Korea*
E-mail: jhyu@kier.re.kr
[b] *Department of Material Science and Engineering, Chungnam National University, Daejeon 305-764, Republic of Korea*

1 X. Dong, W. Jin and N. Xu and K. Li, *Chem. Commun.,* 2011, **47**, 10886-10902.
2 S. Baumann, W.A. Meulenberg and H.P. Buchkremer, *J. Eur. Ceram. Soc.,* 2013, **33**, 1251-1261.
3 X. Zhu, H. Liu, Y. Cong and W. Yang, *Chem. Commun.,* 2012, **48**, 251-253.
4 Y. Liu, X. Zhu, M. Li, H. Liu, Y. Cong and W. Yang, *Angew. Chem. Int. Ed*., 2013, **52**, 3232-3236.
5 H. Luo, K. Efimov, H. Jiang, A. Feldhoff, H. Wang and J. Caro, *Angew. Chem. Int. Ed*., 2011, **50**, 759-763.
6 I. G. Torregrosa, M. P. Lobera, C. Solís, P. Atienzar and J.M. Serra, *Adv. Energy Mater*., 2011, **1**, 618-625.
7 Z. Shao, W. Yang, Y. Cong, H. Dong, J. Tong and G. Xiong, *J. Membr. Sci.,* 2000, **172**, 177-188.
8 Z. Shao and S.M. Haile, *Nature,* 2004, **431**, 170-173.
9 F. Schulze-Küppers, S. Baumann, W.A. Meulenberg, D. Stöver and H.-P. Buchkremer, *J. Membr. Sci*., 2013, **433**, 121-125.
10 K. Watenabe, M. Yuasa, T. Kida, Y. Teraoka, N. Yamazoe and K. Shimanoe, *Adv. Mater*., 2010, **22**, 2367-2370.
11 H. Wang, C. Tablet, A. Feldhoff and J. Caro, *Adv. Mater*., 2005, **17**, 1785-1788.
12 M. Arnold, H. Wang and A. Feldhoff, *J. Membr. Sci.,* 2007, **293**, 44-52.
13 A.Waindich, A. Möbius and M. Müller, *J. Membr. Sci.,* 2009, **337**, 182-187.
14 T. Liu, Y. Wang, R. Yuan, J. Gao, C. Chen and H.J.M. Bouwmeester, *ACS Appl. Mater. Interfaces,* 2013, **5**, 9454-9460.
15 J.H. Joo, G. S. Park, C.-Y. Yoo and J. H. Yu, *Solid State Ionics,* 2013, **253** (2004) 64-69.
16 H. Luo, H. Jiang, T. Klande, Z. Cao, F. Liang, H. Wang and J. Caro, *Chem. Mater.,* 2012, **24**, 2148-2154.
17 A.L. Shaula, V.V. Kharton, F.M.B. Marques, A.V. Kovalevsky, A.P.

Viskup and E.N. Naumovich, *J. Solid State Electrochem*., 2006, **10**, 28-40.
18 V.V. Kharton, A.V. Kovalevsky, A.P. Viskup, F.M. Figueiredo, A.A. Yaremchenko, E.N. Naumovich and F.M.B. Marques, *J.Electrochem. Soc*., 2000, **147**, 2814-2821.
19 J. Yi, Y. Zuo, W. Liu and L. Winnubst, C. Chen, *J. Membr. Sci*., 2006, **280**, 849-855.
20 K. Zhang, Z. Shao, C. Li and S. Liu, *Energy Environ. Sci.,* 2012, **5**, 5257-5264.
21 K. Zhang, L. Liu, Z. Shao, R. Xu, J.C.D. da Costa, S. Wang and S. Liu, *J. Mater. Chem. A.,* 2013, **1**, 9150-9156.
22 H. Hayashi, M. Kanoh, C.J. Quan, H. Inaba, S. Wang, M. Dokiya and H. Tagawa, *Solid State Ionics,* 2000, **132**, 227-233.
23 S. Imashuku, L Wang, K. Mezghani, M. A. Habib, Y. Shao-Horn, 2013, **160 (11)**, E148-E153.
24 V.V. Kharton, A.V. Kovalevsky, A.P. Viskup, F.M. Figueiredo, A.A. Yaremchenko, E.N. Naumovich and F.M.B. Marques, *J. Electrochem. Soc.*, 2000, **147**, 2814-2821.
25 J. Fleig, H.-R. Kim, J. Jamnik and J. Maier, *Fuel Cells*, 2008, **8**, 330-337.
26 J.H. Joo and G.M. Choi, *J. Eur. Ceram. Soc.*, 2007, **27**, 4273-4277.
27 J. Mizusaki, Y. Yonemura, H. Kamata, K. Ohyama, N. Mori, H. Takai, H. Tagawa, M. Dokiya, K. Naraya, T. Sasamoto, H. Inaba and T. Hashimoto, *Solid State Ionics*, 2000, **132**, 167-180.
28 J.H. Joo, R. Merkle, J.-H. Kim and J. Maier, *Adv. Mater*., 2012, **24**, 6507-6512.
29 P. Hjalmarsson, M. Søgaard and M. Mogensen, *Solid State Ionics*, 2008, **179**, 1422-1426.
30 J. Yi, M. Schroeder and M. Martin, *Chem. Mater.*, 2013, **25**, 815-817.
31 H. Luo, K. Efimov, H. Jiang, A. Feldhoff and H. Wang, J. Caro, *Angew. Chem. Int. Ed.*, 2011, **50**, 759-763.

TOC Graphic and text:

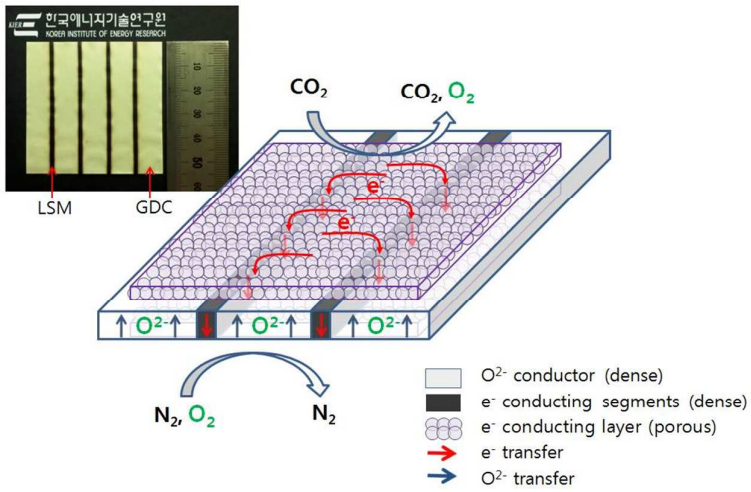

A novel oxygen permeation membrane with tunable segmented configuration with high oxygen permeation is a promising alternative for industrial application in the oxygen production.